PHYSICSAccess Research Paper
ISSN Online: 2756-3898, ISSN Print: 2714-500X https://doi.org/10.47514/phyaccess.2024.4.2.004

Plasmonic Photo-Electrode with AgNPs as Artificial Nano-Antenna for Enhanced Performance in Perovskite Solar Cells

Nicodemus Kure[1], Daniel I Hyuk[1], Eli Danaladi[2] and Dogara M Dary[1]

[1] Department of Physics, Faculty of Sciences, Kaduna State University, Kaduna, Kaduna State, Nigeria
[2] Department of Physics, Federal University of Health Sciences, Otukpo, Benue State, Nigeria

Corresponding E-mail: kurenicodemus@gmail.com

Received 30-07-2024
Accepted for publication 10-09-2024
Published 13-09-2024

Abstract

The introduction of noble metal nanoparticles in solar cells has been proven to enhance the performance of perovskite solar cells. In this study, silver-modified photoanodes were utilized to improve the performance of perovskite solar cells through successive ionic layer adsorption and reaction (SILAR) procedures. Due to the surface plasmon resonance effect, the light trapping capacity of the device was enhanced with superior photovoltaic properties. The plasmonic effects of the introduced silver nanoparticles (AgNPs) were explored using SEM, XRD, UV-visible absorption spectrophotometer and solar simulator. The SEM results show compact morphologies and shinning surfaces indicating the presence of AgNPs. The XRD result shows a good crystal phase. The UV-vis results show enhanced optical absorption with AgNPs incorporation. The photovoltaic characteristics of the fabricated PSCs are: (i) pristine device; Jsc of 6.440 mA/cm^2, Voc. of 0.948 V, FF of 0.642 and PCE of 3.917%, (ii) device with 1 SILAR of AgNPs; Jsc of 014.426 mA/cm^2, Voc. of 0.949 V, FF of 0.642 and PCE of 8.795%, and (iii) device with 2 SILAR of AgNPs; Jsc of 10.815 mA/cm^2, Voc of 0.917 V, FF of 0.558 and PCE of 5.536%. The device with the best performance is made of 1 SILAR cycle of AgNPs which shows an enhancement of ~2.245 times in PCE, ~2.240 times in Jsc and ~1.001 times in Voc over the reference device. The results in this study have unlocked the beneficial role of AgNPs and further contribute to understanding surface plasmon effect due to AgNPs introduction.

Keywords: Silver Nanoparticles; Perovskites Solar Cells; Surface Plasmon; SILAR.

I. INTRODUCTION

Recently, the photovoltaic horizon has witnessed a great revolution due to rapid development in new technology tailored towards perovskite solar cells (PSCs). Since their first development with 3.8% efficiency [1], perovskite solar cells have continued to soar and gain prominence due to their cost effectiveness, low surface recombination rate, high absorption coefficient and mobility of charge carriers, narrow range of exciton binding energy, wide band gap (E_g), long diffusion length and good tolerance towards defects [2-5]. At present, the efficiency has attained a certified value of 26.1% [6].

Despite these record achievements, PSCs are still plagued with many challenges that limit their outdoor applications which include low PCE, disparity in the forward and reverse measurement of current-voltage characteristics [7], and instability in the presence of heat, oxygen, humidity, and UV radiation [8-10]. These limitations contribute immensely to

the non-rooftop application of PSCs despite the competitive state-of-the-art power conversion efficiency in the PV domain.

Several routes have been considered a potential means for the enhancement of the efficiency of PSC with the use of noble metal nanoparticles being a strong candidate. The commonest is embedding nanoparticles in the transport layer, which can increase the roughness and the surface area, thus creating better bonding with the device's active layer and subsequently improving the charge extraction capability [11]. The metal nanoparticle has positive optical effects, this is because it scatters the incoming light in the light-harvesting layer which results in a longer optical path and subsequently improves the probability of absorption [7]. This metal nanoparticle acts as an artificial antenna that results in light trapping in their proximity, and if the absorbing layer has a balanced state of alignment with the nanoparticle, the localized electromagnetic field can directly excite electrons into the conduction band, initiating the photovoltaic effect.

The introduction of metal nanoparticles in the light-harvesting layer, can result in tremendous enhancements in the photocurrent and fill factor. To minimize recombination processes in PSC, it is highly necessary to prevent direct contact of the metal nanoparticles with the active layer, of which the use of a well-controlled oxide shell is required of the metal NPs [12-14]. Reference [15] studied the impact of metal nanoparticles in PSCs. They blended Au@SiO_2 nanoparticles with a core-shell NP in Al_2O_3 film to prepare an Al_2O_3 mesoporous scaffold and fabricated highly porous PSCs, and the average efficiency improved from 8.5 to 9.5%. The increase in the obtained efficiency was attributed to a decrease in the perovskite binding energy in the presence of nano-Au LSPR. Similarly, Luo *et al.* [16], demonstrated an enhancement in PCE from 12.59 to 18.24% by simply introducing Au@TiO_2 nanospheres to enhance the generation rate of charge careers and the probability of career separation and facilitate carrier transfer in the device. Many other studies have also shown improvement with the introduction of metal nanoparticles [4, 6, 17-19], however, the process results in high recombination kinetics, due to direct exposure of the perovskite layer with the metal nanoparticles. This problem makes it difficult to use AgNPs in PSCs; as a result, a suitable synthesis and deposition approach that has no negative effects on the perovskite layer is preferred to make it practical for usage.

Motivated by the stated limitation above, this present work was conducted to investigate the utilization of AgNPs in perovskite solar cells. To prevent recombination processes in the device, we used SiO_2 as a protective shell to avoid direct contact of AgNPs with the absorbing layer. This entire work is categorized into four parts. After the introductory section, the methodology section gives a full description related to the synthesis and fabrication of the benign devices. The third section includes the results and discussion while the fourth section is made up of a summary of the findings from the study.

II. MATERIALS AND METHODS

A. Materials

The main materials used include Ti-Nanoxide Tsp-36, Methanol (SIGMA-ALDRICH 99.8%), Tin II chloride (SIGMA-ALDRICH), Ammonium hydroxide (BDH), Silver nitrate (BDH), Tin granules (BDH), Sodium hydroxide (BDH), Fluorine Doped Tin Oxide (FTO) (SOLARONIX), distilled water, Titanium tetrachlorate (BDH), butyrolactone (GBL), dimethylsulfoxide (DMSO), Sodium Laureth Sulphate, Methanol and Ethanol (SIGMA ALDRICH), Titanium Isopropoxide (SIGMA ALDRICH), Methyl Ammonium Iodide (MAI) (SOLARONIX), titanium nanoxide D/SP (SOLARONIX), Acetyl Acetone (BDH), Lead Iodide Powder (SIGMA ALDRICH), N, N-dimethylformamide (DMF) (SIGMA ALDRICH), Lead II Oxide 99% (SIGMA ALDRICH), TiO_2 paste (DYESOL 18NR-T), SiO_2 (SOLARONIX), and Elcocarb B/SP (SOLARONIX).

B. Equipments

The main equipment includes Muffle furnace, UV-Vis-NIR spectrophotometer, electric hand engraver (Swisso 220/250 VAC), magnetic stirrer plate, IR thermometer, Sonicator, forceps, Keithley 2400 source meter, Scanning Electron Microscope (SEM), Squeegee, Industrial Hot Plate, beakers, sharp tweezers, glass knife, air dryer, XRD (Rigaku D, Max 2500, Japan).

C. Preparation of the Cationic Precursor

The AgNPs were prepared following a method earlier described by Thomas *et al*. [20], this involved dissolving 0.05 g of silver nitrate in 30 ml of deionised water. Ammonium hydroxide (NH_4OH) was added dropwise. With a small amount of NH_4OH, a brownish precipitate appears which results in silver (I) oxide ($Ag_2O_{(s)}$) formation. With an excess of NH_4OH to silver (I) oxide ($Ag_2O_{(s)}$), a colourless solution of diamine silver complex ion was formed.

D. Preparation of anionic precursor

To prepare the anionic precursor, 0.1 m (1.13g) Tin (II) chloride was added to 50 ml of distilled water resulting in insoluble $Sn(OH)Cl_{(s)}$.

E. Synthesis of mesoporous TiO_2

The TiO_2 was prepared by dispersing TiO_2 paste (Dyesol 18NR-T) in methanol (TiO_2 to methanol ratio is 1:3) at room temperature. This reduces the TiO_2 paste thickness.

F. Preparation of Methyl Ammonium Lead Tri-Iodide Perovskite ($MAPbI_3$) Precursors

This was prepared following a method earlier described by Danladi *et al*. [4]. Precursor A (PbI_2): Dimethyl formamide was combined with 4.6 g of lead iodide (PbI_2). This combination was heated at 250 ℃ for 45 minutes in a bath of molten wax.

Precursor B (MAI): 0.3 g of methyl ammonium iodide and 20 ml of dried isopropanol were combined and shaken for 3

minutes until equilibrium was reached without any remaining white residue.

G. Photoanode preparation

Sodium laureth sulphate was used to clean fluorine-doped Tin Oxide (FTO). The compact TiO_2 was used as received at its analytical grade level. The compact TiO_2 was deposited using the screen printing technique, where a 120-mesh device was used to directly screen print Ti-Nanoxide D/SP on FTO. It was dried at 150 ℃ for 10 minutes, then annealed at 450 ℃ for 30 minutes. The mesoporous TiO_2 was deposited on the c-TiO_2 using spin coating at 4000 rpm for 20 seconds. For the pristine device, a few drops of the prepared Precursor A were dynamically spin-coated, and then Precursor B was spin-coated on the precursor A. A dark perovskite layer was formed, and it was placed in a beaker of dry propanol for five minutes, this was used to remove any extra MAI. The photoanode made of FTO/c-TiO_2/m-TiO_2/$MAPbI_3$ was annealed at 120 ℃ for 10 minutes. For the second and third devices, 1 and 2 SILAR cycles of AgNPs were deposited between the m-TiO_2 and $MAPbI_3$. This was done as follows; the FTO containing the c-TiO_2 and m-TiO_2 was dipped in $[Ag(NH_3)_2]^+$solution for 2 minutes which describes the adsorption process, then rinsed with distilled water for 1 minute to remove excess adsorbed ions from the diffusion layer, thereafter, it was transferred to the tin chloride solution for 2 minutes which describes the reduction process. The film turns brownish due to the reduction of Ag ions. It was rinsed in distilled water for 1 minute to remove excess unreacted species. This process is called one SILAR cycle. The process was repeated for the device with 2 SILAR cycles, thereafter a thin layer of SiO_2 was coated on the AgNPs.

H. Preparation of Counter Electrode

The material used was a composite made of graphite and carbon black (CGC) in a ratio of 1:3. The CGC was sliced into a rectangle measuring 1 cm^2 in area.

I. Assembly of the Cells

The three photoanodes and the counter electrodes were sealed with ethylene-vinyl acetate to form the three PSCs. The schematic of the cell is shown in Fig. 1.

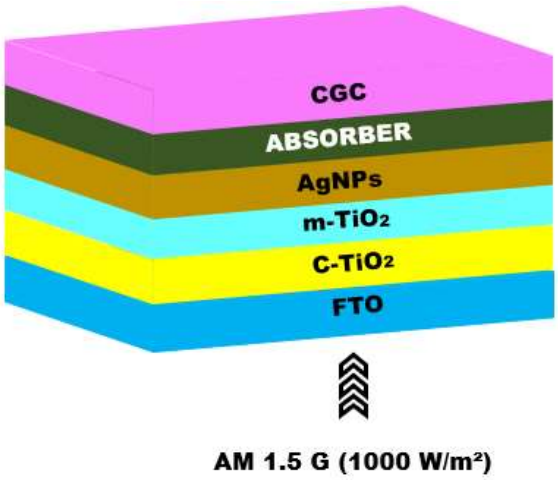

Fig. 1. Schematic diagram of the PSC device.

J. Characterization and Measurement

UV-vis spectroscopy was performed using Axiom Medicals (UV752 UV-Vis-NIR spectrophotometer), the crystal peaks detection was performed using X-ray diffractometer (Rigaku D, Max 2500), Scanning Electron Microscopy (SEM) was performed using Phonon Pro X model. The current-voltage measurement was carried out using a set-up made of a Xenon lamp and a filter coupled in a Keithley-2400 source meter at a 100 mW/cm^2 illumination irradiance.

III. Result and Discussions

A. SEM study

The SEM image of pure TiO_2 film is shown in Fig. 2(a). All the NPs samples used in this study have morphologies that are well-dispersed and nearly spherically porous. The surface of the TiO_2 is dense and without shining particles, which shows that it can create adequate space for the infiltration of the perovskite precursors. Fig. 2(b, c) shows the micrographs of TiO_2 coated with 1 and 2 SILAR cycles of AgNPs. The top surface of m-TiO_2 shows the distribution of AgNPs. The shining surface and the particles dispersed show the capacity of AgNPs to enhance scattering effects and decrease recombination processes. This shows that the addition of AgNPs enhances nucleation and increases the rate of film growth.

B. X-ray analysis

The XRD pattern for TiO_2, TiO_2 with 1 SILAR cycle of AgNPs, and TiO_2 with 2 SILAR cycles of AgNPs are depicted in Fig. 3(a-c). As it is observed, all peaks confirmed the formation of a tetragonal anatase TiO_2 phase. The major peaks

at the 2 theta (2θ) angle of 25.42°, 37.95°, 48.29°, 54.10°, 55.38°, and 62.46° corresponds to the planes (101), (112), (200), (105), (211), and (204) respectively. The peaks and planes depict an excellent match with standard JCPDS card No. 89-4921 and agree with the research work of Danladi *et al*. [4] and Manju and Jawhar [21]. From the peaks, it can be shown that additional peaks due to AgNPs were not present which is clear evidence of the formation of AgNPs-embedded anatase titania nanocomposite.

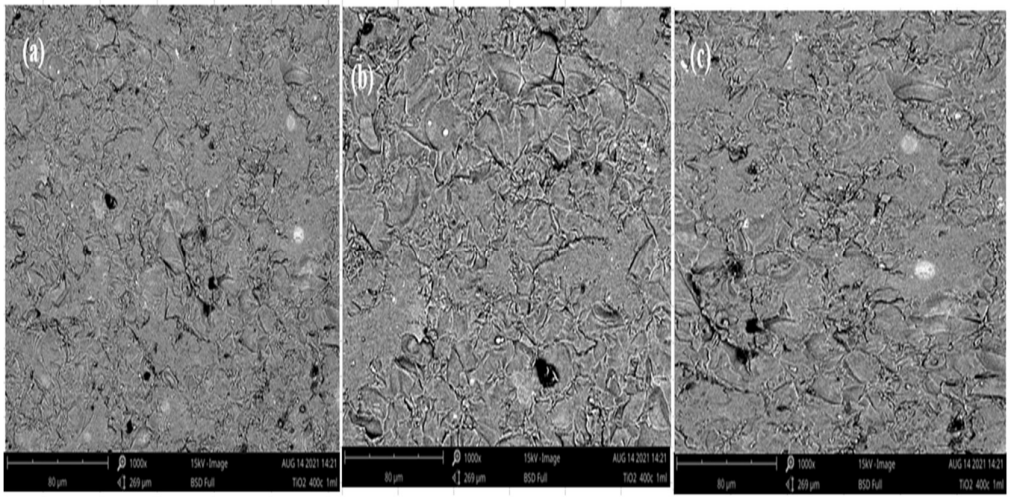

Fig. 2. SEM image of (a) TiO_2 (b) TiO_2 with 1 SILAR cycle and (c) TiO_2 with 2 SILAR cycles.

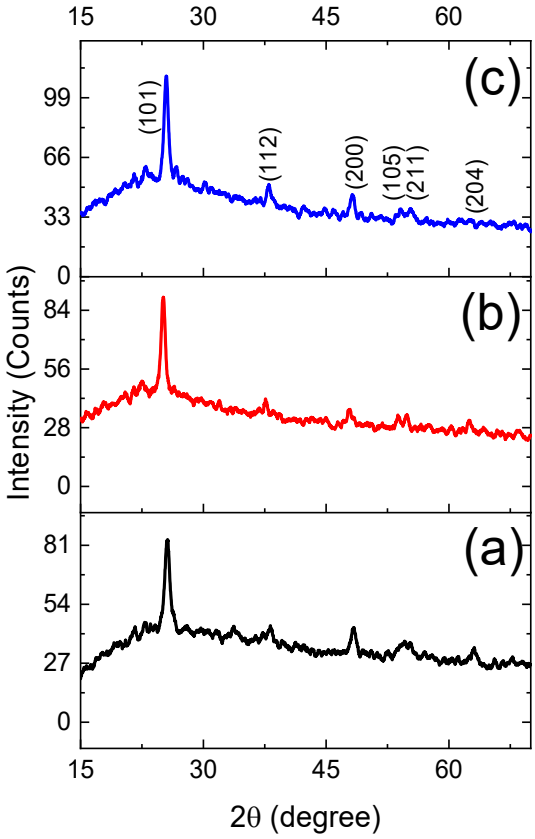

Fig. 3. XRD pattern of (a) TiO_2, (b) TiO_2 with 1 SILAR cycle of AgNPs, and (c) TiO_2 with 2 SILAR cycles of AgNPs.

C. Optical study

Fig. 4a shows the absorption curve of pure TiO_2, TiO_2 with 1 SILAR cycle of AgNPs, and TiO_2 with 2 SILAR cycles of AgNPs within the wavelength range of 300-1000 nm. As can be observed in the TiO_2 spectrum, no peak was noticed within the visible region, but a sharp peak was observed around 342 nm. The peak in the UV region of the electromagnetic spectrum is attributed to the strong interaction between O 2p and Ti 3d charges [22]. This suggests that modification of TiO_2 is necessary to make it active in the visible region which is the region of interest in solar cells. The modification of the TiO_2 with AgNPs shows a wide and broad band with a visible peak noticed at 443 nm which corresponds to the surface plasmon resonance (SPR) effect of AgNPs [4, 23-26]. The SPR effect is due to the mutual oscillation of conduction electrons which are in resonance with the light wave [27].

Fig. 4b shows the transmittance versus wavelength of pure TiO_2, TiO_2 with 1 SILAR cycle of AgNPs, and TiO_2 with 2 SILAR cycles of AgNPs within the wavelength range of 300-1200 nm. As depicted from the curve, all the samples show high transparency in the visible and near-infrared region with a fall noticed within the ultraviolet region. The transmittance was pronounced in pure TiO_2 which implies that, the introduction of AgNPs on TiO_2 results into increase in the film porosity [4]. Surface defects, which cause disparity in surface morphology, crystal size, and transmittance to light scattering, are responsible for the observed variations in the film's transmittance [4].

Fig. 4c shows the optical reflectance of pure TiO_2, TiO_2 with 1 SILAR cycle of AgNPs, and TiO_2 with 2 SILAR cycles of AgNPs within the wavelength range of 300-1200 nm. As

demonstrated in the curve, the photoanodes were observed to be relatively reflective. The reflectance was seen to decrease with an increase in the SILAR cycle. The reflectance shows a valley and peak which is attributed to the increase in surface roughness [27].

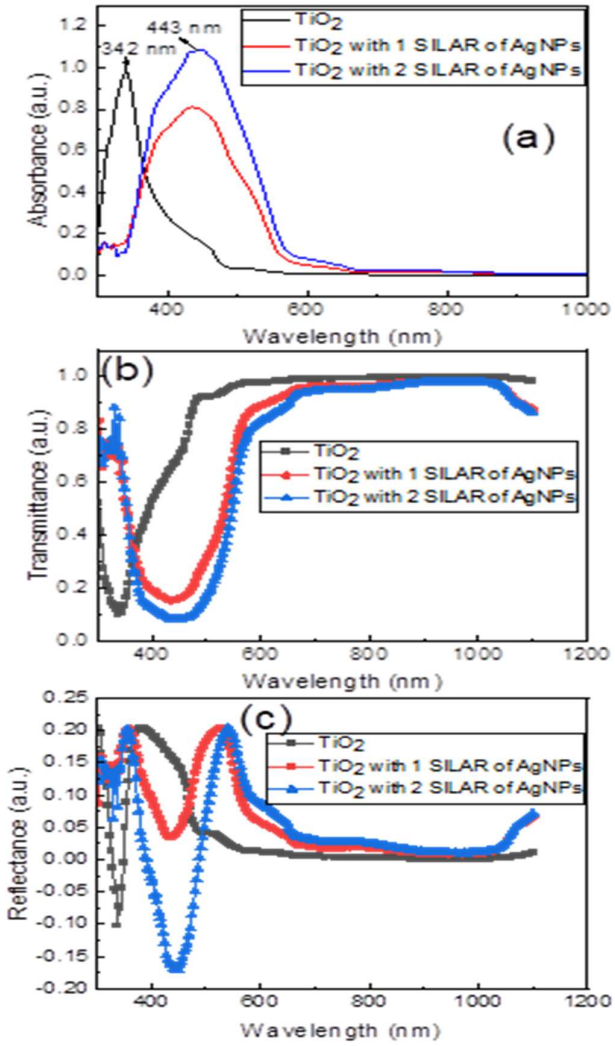

Fig. 4. (a) absorbance of TiO_2, TiO_2 with 1 SILAR cycle of AgNPs, and TiO_2 with 2 SILAR cycles of AgNPs, (b) transmittance of TiO_2, TiO_2 with 1 SILAR cycle of AgNPs, and TiO_2 with 2 SILAR cycles of AgNPs and (c) reflectance of TiO_2, TiO_2 with 1 SILAR cycle of AgNPs, and TiO_2 with 2 SILAR cycles of AgNPs.

D. Current-voltage characteristics

To verify the positive influence of surface plasmon resonance on the photovoltaic parameters of solar cells, two AgNPs modified perovskite solar cells were fabricated and their electrical properties were evaluated under AM 1.5 G illumination condition of 100 mW/cm^2. The metric parameters such as open circuit voltage (V_{oc}), short circuit current density (J_{sc}), fill factor (FF) and power conversion efficiency (PCE), were computed from the *J-V* characteristic curve shown in Fig. 5a. The P-V characteristics are depicted in Fig. 5(b), while the correlation between PCE with various device, FF with various device, J_{sc} with various device and V_{oc} with various device is shown in Fig. 6(a-d). Table I summarises the obtained PV data. The pristine PSC device demonstrated a PCE of 3.917%, J_{sc} of 6.440 mA/cm^2, V_{oc} of 0.948 V, and FF of 0.642. All the PSCs with AgNPs inclusion show superior performance over the reference device lacking AgNPs. For the benefit of clarification, the device without AgNPs is labelled as A, while the devices with 1 SILAR and 2 SILAR cycles of AgNPs are labelled as B and C.

Table I. *J-V* characteristic parameters of the devices.

Device	PCE (%)	*FF* (%)	J_{sc} (mA/cm^2)	V_{oc} (V)
A	3.917	0.642	6.440	0.948
B	8.795	0.642	14.426	0.949
C	5.536	0.558	10.815	0.917

When 1 SILAR cycle of AgNPs is utilized in the PSC device, the PCE improves from 3.917 to 8.795% and the J_{sc} increases from 6.440 to 14.426 mA/cm^2. When 2 SILAR cycles of AgNPs are deposited, the device shows a PCE of 5.536%, a J_{sc} of 10.815 mA/cm^2, a V_{oc} of 0.949 V, and an FF of 0.558. The best-performing device is with 1 SILAR cycle. However, all devices with AgNPs outperformed the controlled device. This dramatic increase in PCE and J_{sc} of the device with 1 SILAR cycle is attributed to the enhanced light absorption and broadened light absorption range of the perovskite nanocrystal resulting from the SPR effect of the metallic Ag nanoparticles. The presence of the AgNPs stimulates the generation of charge carriers in the absorber layer. AgNPs have long been considered to be active catalytically [4, 6]. The catalytic actions are displayed when AgNPs are dispersed on metal oxide [27]. In this present work, the presence of AgNPs on the TiO_2 support enhances bond formation between TiO_2 and $CH_3NH_3PbI_3$, thereby improving electron mobility, and giving rise to improved electrical parameters. This improved characteristic speculates that the electrical effects of SPR boost the photoelectric response. Further increase in the number of SILAR from 1 to 2 cycles deteriorates the device performance, which can be attributed to partial coverage of the scaffold which causes the perovskite absorber to have a negative impact on some of the uncoated AgNPs in the Ag-TiO_2 network structure. This functions as the centre of recombination, which limits the number of electron-hole pairs and degrades the device, consequently enhancing the chances of recombination.

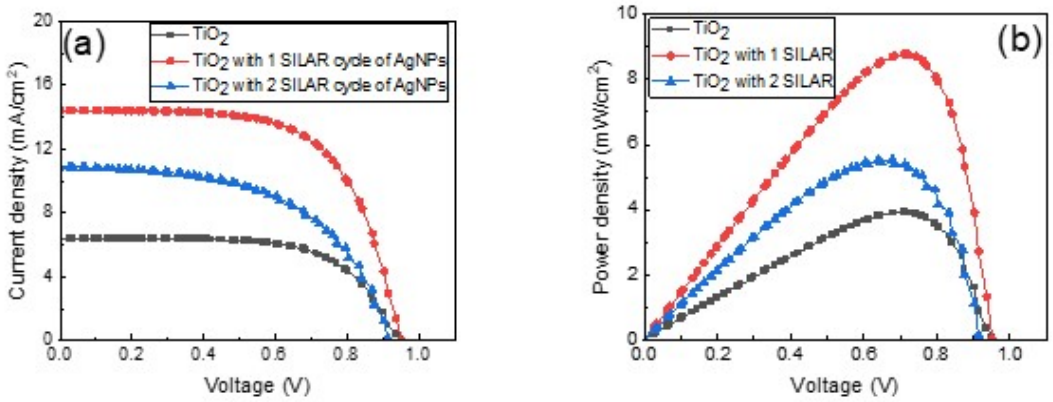

Fig. 5. (a) J–V curves of the device with TiO_2, TiO_2 with 1 SILAR cycle of AgNPs, and TiO_2 with 2 SILAR cycles of AgNPs, and (b) P-V curves of the device with TiO_2, TiO_2 with 1 SILAR cycle of AgNPs, and TiO_2 with 2 SILAR cycles of AgNPs.

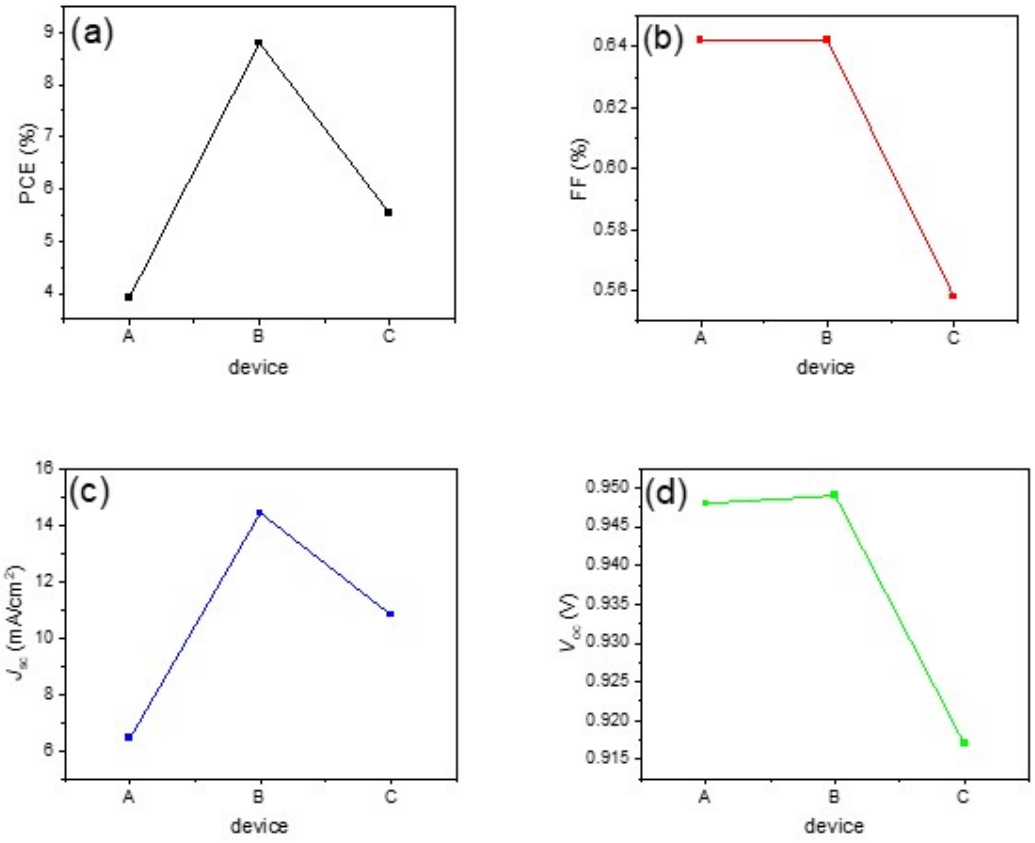

Fig. 6. Correlation between (a) PCE with various devices, (b) FF with various devices, (c) Jsc with various devices and (d) Voc with various devices.

IV. CONCLUSION

In this study, the effects of metallic Ag nanoparticles were investigated on the optical, structural and electrical properties of perovskite solar cells. Different SILAR cycles of AgNPs were introduced into the PSC device. From the results of the study, the following findings were reached; All peaks confirmed the formation of a tetragonal anatase TiO_2 phase and additional peaks due to AgNPs were not present which is clear evidence of the formation of AgNPs-embedded anatase titania nanocomposite. A wide and broadband visible peak at 443 nm was observed when AgNPs were added, which

corresponds to the surface plasmon resonance (SPR) effect of AgNPs. With 1 SILAR cycle of AgNPs, the best device was achieved, which shows a PCE of 8.795%, J_{sc} of 14.426 mA/cm^2, Voc of 0.949 V and FF of 0.650. This shows an improvement of ~2.245 times in PCE, ~2.240 times in *J*sc and ~1.001 times in V_{oc}. The outcome of this research has paved the way for broadband enhancement of PSC devices.

ACKNOWLEDGEMENT

This research was fully funded by Institutional Based Research (IBR) of the Tertiary Education Trust Fund (TETFUND) of Nigeria through Kaduna State University.

Reference

[1] A. Kojima, K. Teshima, Y. Shirai, T. Miyasaka, "Organometal Halide Perovskites as Visible-Light Sensitizers for Photovoltaic Cells", J. Am. Chem. Soc., vol. 131, no. 17, pp. 6050−6051. 2009. https://doi.org/10.1021/ja809598r.

[2] S. Luo, W.A. Daoud, "Recent progress in organic-inorganic halide perovskite solar cells: mechanisms and material design", J. Mater. Chem. A, vol. 3, no. 17, pp. 8992–9010. 2015. https://doi.org/10.1039/C4TA04953E.

[3] E. Danladi, A.C. Egbugha, R.C. Obasi, N.N. Tasie, C.U. Achem, I.S. Haruna, L.O. Ezeh, "Defect and doping concentration study with series and shunt resistance influence on graphene-modified perovskite solar cell: A numerical investigation in SCAPS-1D framework" J. Indian Chem. Soc., vol 100, pp. 101001. 2023. https://doi.org/10.1016/j.jics.2023.101001.

[4] E. Danladi, A. Ichoja, E.D. Onoja, D.S. Adepehin, E.E. Onwoke, O.M. Ekwu, D.O. Alfred, "Broad-Band-Enhanced and Minimal Hysteresis Perovskite Solar Cells with Interfacial Coating of Biogenic Plasmonic Light Trapping Silver Nanoparticles", Mater. Res. Innov., vol. 27, no. 7, pp. 521-536. 2023. https://doi.org/10.1080/14328917.2023.2204585.

[5] G. Giorgi, K. Yamashita, "Organic-inorganic halide perovskites: an ambipolar class of materials with enhanced photovoltaic performances", J. Mater. Chem. A, vol. 3, no. 17, 8981–8991. 2015. https://doi.org/10.1039/C4TA05046K.

[6] E. Danladi, M.Y. Onimisi, S. Garba S, J. Tasiu, "9.05% HTM free perovskite solar cell with negligible hysteresis by introducing silver nanoparticles encapsulated with P_4VP Polymer", SN Appl. Sci., vol. 2, no. 1769. 2020. https://doi.org/10.1007/s42452-020-03597-y.

[7] F. Bastianini, A.I.C. Hidalgo, D.Z. Hook, J.A. Smith, D.Cumming, A. Dunbar, "Using Ag nanoparticles in the electron transport layer of perovskite solar cells to improve efficiency". Sol. Energy, vol. 268, pp. 112318. https://doi.org/10.1016/j.solener.2024.112318.

[8] Z. Qu, F. Ma, Y. Zhao, J. You, "Updated Progresses in Perovskite Solar Cells", Chin. Phys. Lett., vol. 38, no. 10, pp. 107801. 2021. https://doi.org/10.1088/0256-307X/38/10/107801.

[9] C. Zhi, Z. Li, B. Wei, "Recent progress in stabilizing perovskite solar cells through two-dimensional modification", APL Mater., vol. 9, no. 7, pp. 070702. 2021. https://doi.org/10.1063/5.0056106.

[10] T.Y. Yang, N.J. Jeon, H.W. Shin, S.S. Shin, Y.Y. Kim, J. Seo "Achieving Long-Term Operational Stability of Perovskite Solar Cells with a Stabilized Efficiency Exceeding 20% after 1000 h", Adv. Sci., vol. 6, no. 14, pp. 1900528. 2019. https://doi.org/10.1002/advs.201900528.

[11] S. Woo, J. Jeong, H. Lyu, Y. Han, Y. Kim, "*In situ*-prepared composite materials of PEDOT: PSS buffer layer-metal nanoparticles and their application to organic solar cells", Nanoscale Res. Lett., vol. 7 pp. 641. 2012. https://doi.org/10.1186/1556-276X-7-641.

[12] Y.F. Li, Z.L. Kou, J. Feng, H.B. Sun, "Plasmon-enhanced Organic and Perovskite Solar Cells with Metal Nanoparticles", Nanophotonics, vol. 9, no. 10, pp. 3111−3133. 2020. https://doi.org/10.1515/nanoph-2020-0099.

[13] K. Yao, H.J. Zhong, Z.L. Liu, M. Xiong, S. Leng, J. Zhang, Y.X. Xu, W. Wang, L. Zhou, H. Huang, A.K.Y. Jen, "Plasmonic Metal Nanoparticles with Core-Bishell Structure for High-Performance Organic and Perovskite Solar Cells", ACS Nano, vol. 13, no. 5, pp. 5397−5409. 2019. https://doi.org/10.1021/acsnano.9b00135.

[14] E.S. Arinze, B. Qiu, G. Nyirjesy, S.M. Thon, "Plasmonic Nanoparticle Enhancement of Solution-Processed Solar Cells: Practical Limits and Opportunities", ACS Photonics, vol 3, no. 2, pp. 158−173. 2016. https://doi.org/10.1021/acsphotonics.5b00428.

[15] Zhang W, Saliba M, Stranks SD, Y. Sun, X. Shin, U. Wiesner, H.J. Snaith, "Enhancement of Perovskite-based Solar Cells Employing Core-shell Metal Nanoparticles", Nano Lett., vol. 13, no. 9, pp. 4505−4510. 2013. https://doi.org/10.1021/nl4024287.

[16] Q. Luo, C. Zhang, X. Deng, H. Zhu, Z. Li, Z, Wang, X. Chen, X. Huang, "Plasmonic Effects of Metallic Nanoparticles on Enhancing Performance of Perovskite Solar Cells", *ACS Appl. Mater. Interfaces,* vol. 9, no. 40, pp. 34821−34832. 2017. https://doi.org/10.1021/acsami.7b08489.

[17] L. Zhang, T. Liu, L. Liu, M. Hu, Y. Yang, A. Mei, H. Han, "The effect of carbon counter electrodes on fully printable mesoscopic perovskite solar cells", J Mater Chem A., vol. 3, no. 17, pp. 9165-9170. 2015. https://doi.org/10.1039/C4TA04647A.

[18] B. Ai, Z. Fan, Z.J. Wong, "Plasmonic–perovskite solar cells, light emitters, and sensors", Microsyst.

Nanoeng., Vol. 8, no. 5. 2022. https://doi.org/10.1038/s41378-021-00334-2.

[19] M. Saliba, W. Zhang, V.M. Burlakov, S.D. Stranks, Y. Sun, J.M. Ball, M.B. Johnston, A. Goriely, U. Wiesner, H.J. Snaith, "Plasmonic-Induced Photon Recycling in Metal Halide Perovskite Solar Cells", Adv. Funct. Mater., vol. 25, no. 31, pp. 5038-5046. 2015. https://doi.org/10.1002/adfm.201500669.

[20] D. Thomas, E. Danladi, M.T. Ekwu, P.M. Gyuk, M.O. Abdulmalik, I.O Echi, "Effect of Silver Nanoparticles SILAR Cycle on TiO2 Nanoparticles Thin Film: Optical and Structural Study",. East Euro. J. Phy., vol. 2022, no. 4, pp. 118-124. 2022. https://doi.org/10.26565/2312-4334-2022-4-11.

[21] J. Manju, S.M.J. Jawhar, "Synthesis of magnesium-doped TiO_2 photoelectrodes for dye-sensitized solar cell applications by solvothermal microwave irradiation method", J. Mater. Res., vol. 33, no. 11, pp. 1534-1542. 2018. https://doi.org/10.1557/jmr.2018.115.

[22] F. Ahmed, M.B. Kanoun, C. Awada, C. Jonin, P. F. Brevet, Crystals, "An Experimental and Theoretical Study on the Effect of Silver Nanoparticles Concentration on the Structural, Morphological, Optical, and Electronic Properties of TiO_2 Nanocrystals", vol. 11, no. 12, pp. 1488. 2021. https://doi.org/10.3390/cryst11121488.

[23] V. Katta, and R. Dubey, "Green synthesis of silver nanoparticles using Tagetes erecta plant and investigation of their structural, optical, chemical and morphological properties" Materials Today: Proceedings, vol. 45, pp. 794-798. 2021. https://doi.org/10.1016/j.matpr.2020.02.809.

[24] M.G. González-Pedroza, A.R.T. Benítez, S.A. Navarro-Marchal, E. Martinez-Martinez, J.A. Marchal, H. Boulaiz, R.A. Morales-Luckie, "Biogeneration of silver nanoparticles from *Cuphea procumbens* for biomedical and environmental applications", Sci. Rep., vol. 13, pp. 790. 2023. https://doi.org/10.1038/s41598-022-26818-3.

[25] M. Madani, S. Hosny, D. M. Alshangiti, N. Nady, S. A. Alkhursani, H. Alkhaldi, S. A. Al-Gahtany, M. M. Ghobashy, and G. A. Gaber, Green synthesis of nanoparticles for varied applications: Green renewable resources and energy-efficient synthetic routes", Nanotechnol. Rev., vol. 11, no. 1, 731 (2022). https://doi.org/10.1515/ntrev-2022-0034.

[26] Y. Khane, K. Benouis, S. Albukhaty, G. M. Sulaiman, M. M. Abomughaid, A. Al Ali, D. Aouf, F. Fenniche, S. Khane, W. Chaibi, A. Henni, H. D. Bouras, and N. Dizge, "Green Synthesis of Silver Nanoparticles Using Aqueous *Citrus limon* Zest Extract: Characterization and Evaluation of Their Antioxidant and Antimicrobial Properties", Nanomaterials, vol. 12, no. 12, pp. 2013. 2022. https://doi.org/10.3390/nano12122013.

[27] J. Tasiu, M.Y. Onimisi, A.S. Yusuf, E. Danladi, N.N. Tasie, "Effect of Biosynthesized Silver Nanoparticles on The Optical, Structural, and Morphological Properties of TiO_2 Nanocrystals", East Eur. J. Phy., vol. 2024, no. 1, pp. 315-321. 2024. https://doi.org/10.26565/2312-4334-2024-1-28.